Supplementary Information

for

Generation of functional RNAs from inactive oligonucleotide complexes by non-enzymatic primer extension

Katarzyna Adamala, Aaron E. Engelhart and Jack W. Szostak

Supplementary Discussion

Nonenzymatic primer extension in presence of mixed base monomers

As a means of probing the sensitivity of primer-extension based reconstitution of functional RNA activity from partial fragments to the presence of mismatched bases, we examined the malachite green aptamer and hammerhead ribozyme in the presence of all four activated nucleotides: 2MeImpG, 2MeImpC, 2MeImpU and 2MeImpA. Even in the presence of equimolar amounts of each base, the nonfunctional malachite green aptamer containing a truncated primer-length strand yields active aptamer after a 24 hour primer extension reaction (Figure S3). Similarly, when all four monomers are present, hammerhead ribozyme fragments yield active ribozymes after primer extension, in all permutations of primer and template strands (Figure S4).

RNA stability

We examined the UV-monitored thermal stability of the functional RNAs employed (in both full-length and primer, 3‘-truncated forms) in divalent-ion-free conditions, under which observed changes in absorbance would be principally due to secondary (and not tertiary) structure, and the hammerhead ribozyme would not self-cleave. The thermal denaturation traces of the functional RNAs employed exhibit clear stabilization of secondary structure in their full-length forms, relative to their 3‘-truncated primer forms.

The malachite green aptamer, in its primer form, exhibits two transitions, with midpoints of 21 °C and 45 °C (Fig. S5, open triangles). When the full-length stems expected to be formed by primer extension are present, the aptamer exhibits a single, sharp melting transition, with a midpoint at 50 °C (Fig. S5, closed triangles). The hammerhead ribozyme, in its 3‘-truncated primer form (Fig. S5, open diamonds), is largely unstructured, with a broad melting transition centered at 29 °C. In its full-length form, which is capable of forming two additional stems, this transition is shifted upward by ca 40 °C (Fig. S5, closed diamonds). The Diels-Alderase is known to have a high degree of intramolecular structure and exhibits two melting transitions, with the second incomplete even at 95 °C in either form of this highly structured RNA (Fig. S5, circles). The first melting transition, with an apparent midpoint of 18 °C in the 3‘-truncated form of this RNA (Fig. S5, open circles), increases to 38 °C in the full-length form of this RNA (Fig. S5, closed circles); the second partial melting transition also occurs at higher temperature.

Supplementary Figure S1

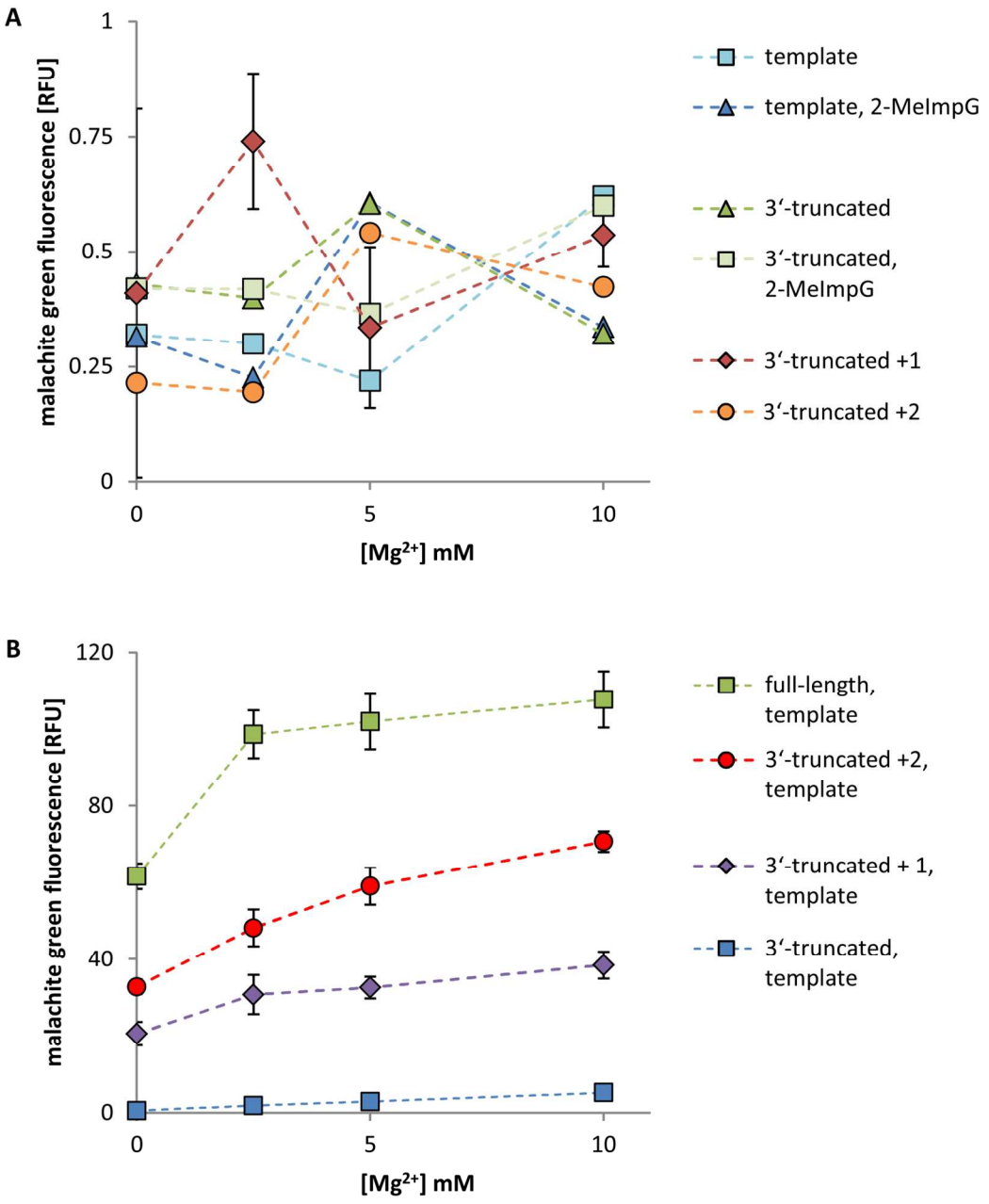

Supplementary Figure S1. Malachite green aptamer.

Both template and full-length 3′-truncated strands are required for maximum malachite green fluorescence, and each successive addition of guanosine residues to the 3′-end of the 3′-truncated strand increases malachite green fluorescence.

A: In the presence of either one of the aptamer strands alone, malachite green fluorescence does not increase, even after incubation with 2-MeImpG. Both primer and template strands are necessary for aptamer reconstitution.
B: In the presence of both 3′-truncated and template strands, malachite green fluorescence increases as the 3′-truncated primer strand is extended. The higher increase of malachite green fluorescence with non-full length 3′-truncated strands (3′-truncated +1 and 3′-truncated +2) at higher magnesium concentrations indicates the importance of duplex stabilization to the activity of the aptamer. Each sample contained 0.25 M Tris-HCl pH 8.0, 0.15 M NaCl, 2 μM malachite green, 1 μM each strand of the aptamer.

Supplementary Figure S2

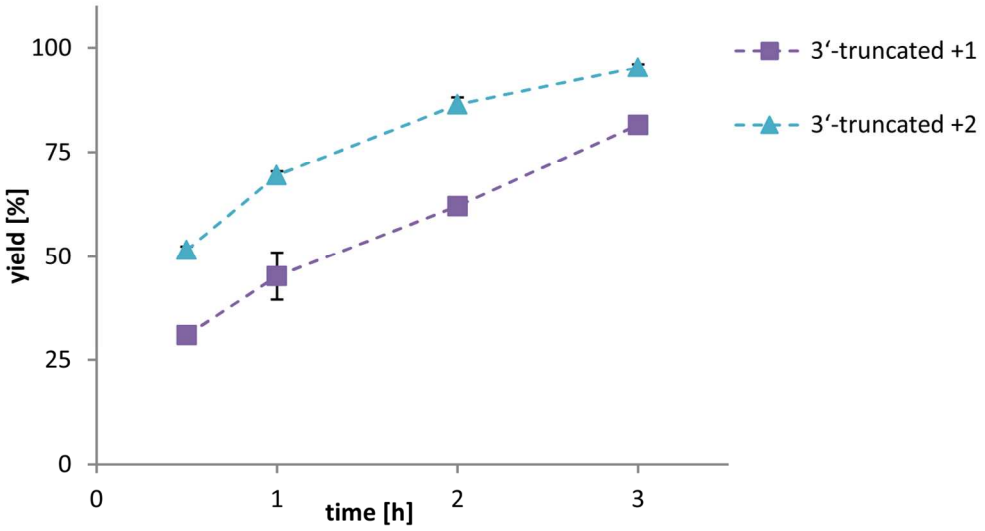

Supplementary Figure S2. Yield of Diels-Alder reactions catalyzed by Diels-Alderase ribozymes with differing numbers of G residues at the 3′-end.

Violet squares: Ribozyme RNA corresponding to the addition of one G to the 3′-truncated ribozyme; blue triangles: Ribozyme RNA corresponding to the addition of 2 bases to the 3′-truncated ribozyme. Reaction conditions: 100 mM Tris-HCl pH 7.5, 100 mM $MgCl_2$, 300 mM NaCl, 200 µM 9-hydroxymethylanthracene, 1000 µM N-propylmaleimide, 10 µM RNA. Each experiment was done in duplicate; error bars indicate extreme values.

Supplementary Figure S3

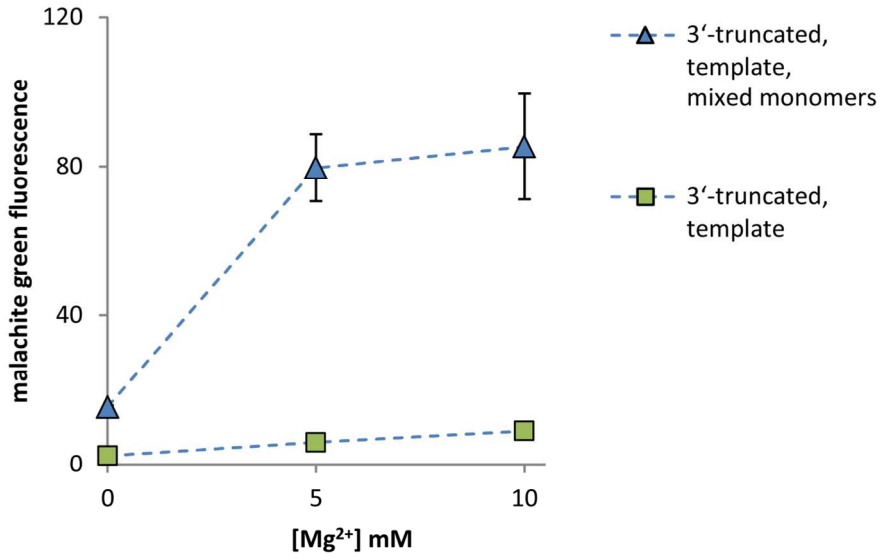

Supplementary Figure S3. The malachite green aptamer with mixed activated RNA monomers

The malachite green 3'-truncated and template strands were subjected to non-enzymatic primer extension in the presence of all four activated nucleotides.

The presence of all four monomers results in an aptamer with comparable activity to that produced in primer extension reactions containing only 2MeImpG, demonstrating that mismatch incorporation is sufficiently low as to not impair the efficacy of this system.

Primer extension using mixed monomers resulted in a 11-fold fluorescence increase of malachite green at 10mM Mg^{2+} (85 RFU after primer extension vs. 8 RFU before), which compares favorably to reactions employing only 2MeImpG, which gave a 13-fold enhancement (107 RFU vs. 8 RFU).

Each primer extension reaction contained 0.25 M Tris-HCl pH 8, 0.15 M NaCl, 5 µM RNA total (2.5 µM each strand), 12.5 mM each of the four activated nucleotides, and 50 mM $MgCl_2$. Primer extension was performed for 24 H. Malachite green fluorescence was examined in reactions containing 0.25 M Tris-HCl pH 8.0, 0.15 M NaCl, 2 µM malachite green, 1 µM each strand of desalted aptamer.

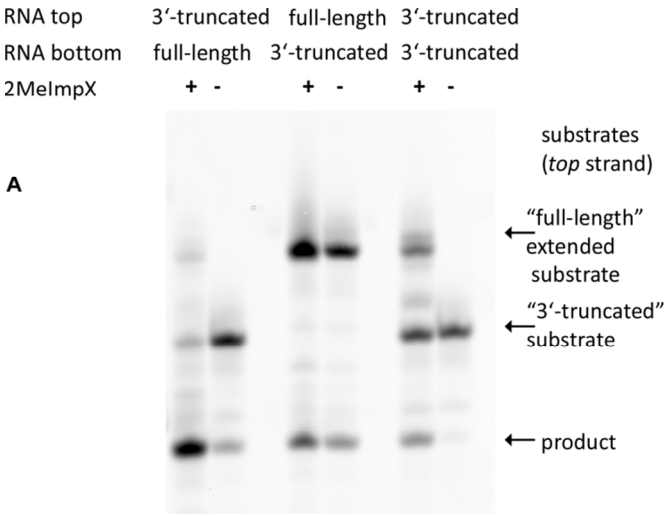

B

Comparison of cleavage yields between reactions containing pure 2MeImpG and those containing a mixture of all 4 RNA monomers (2MeImpX)

RNA top	3′-truncated		full-length		3′-truncated	
RNA bottom	full-length		3′-truncated		3′-truncated	
monomer	+	-	+	-	+	-
2MeImpX	63	20	31	16	23	3
2MeImpG	64	37	33	6	25	5

Supplementary Figure S4. Hammerhead ribozyme with mixed activated RNA monomers

Hammerhead ribozyme 3′-truncated strands were subjected to nonenzymatic primer extension in the presence of all four activated nucleotides.

The presence of all four monomers does not inhibit nonenzymatic primer extension or ribozyme activity, demonstrating that mismatch incorporation is sufficiently low as to not impair the efficacy of this system.

Employing both 3′-truncated top and bottom strands (with no activated monomers) resulted in 3% hammerhead cleavage yield after 24 hrs. The addition of all four 2-methylimidazolides (2MeImpX) resulted in 23% cleavage yield, comparable to that achieved in the presence of only 2MeImpG, which gave 29% cleavage yield (Figure 3). Other configurations of strands gave similar yield enhancements. Cleavage yields for reactions with 2MeImpX and those with 2MeImpG (i.e., data from Figure 3) are given in table in panel B.

Each primer extension reaction contained 0.25 M Tris-HCl pH 8, 0.15 M NaCl, 2.5 μM each RNA strand, 12.5 mM each of the four activated nucleotides, and 50 mM $MgCl_2$. Primer extension was performed for 24 hrs.

Supplementary Figure S5

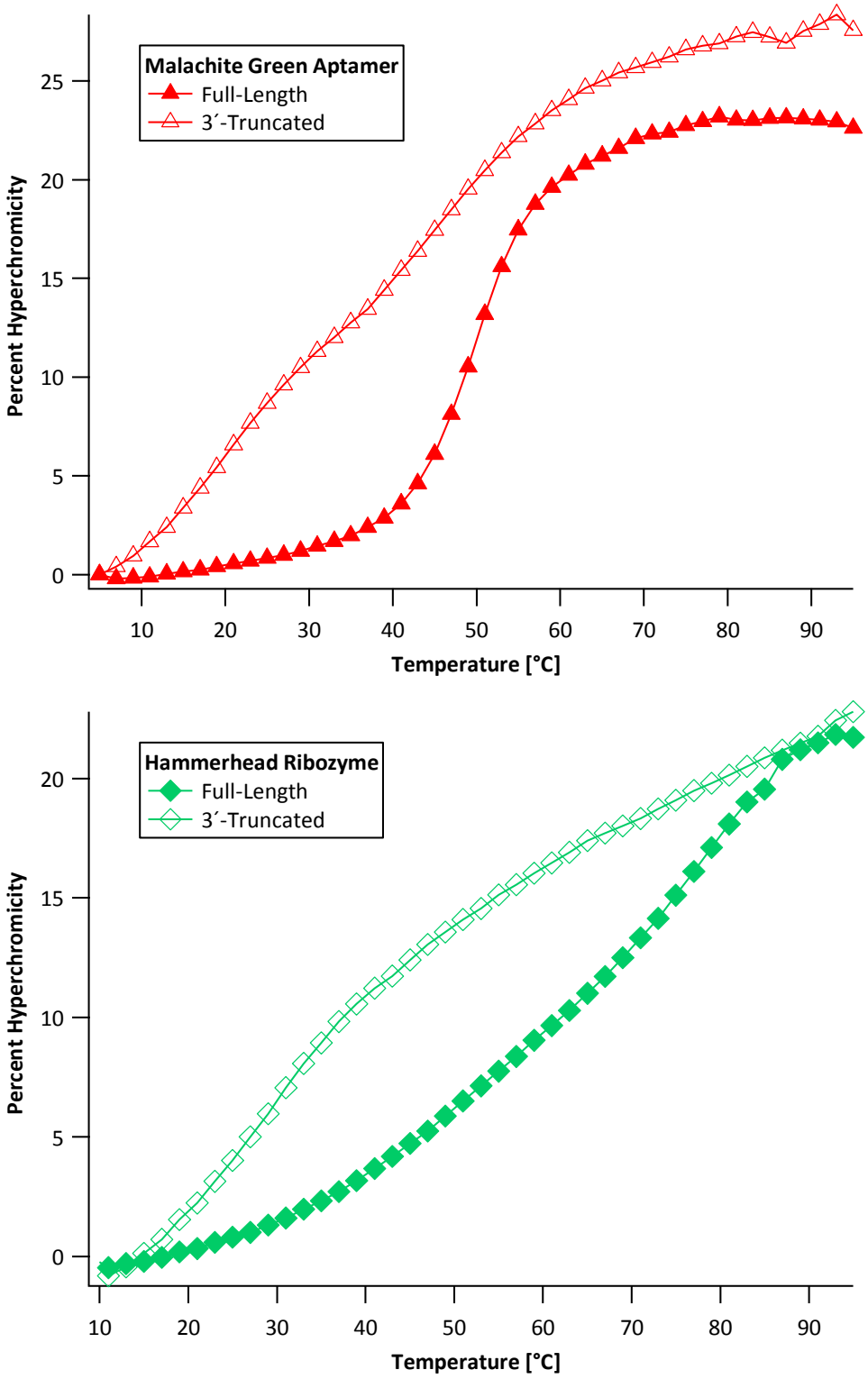

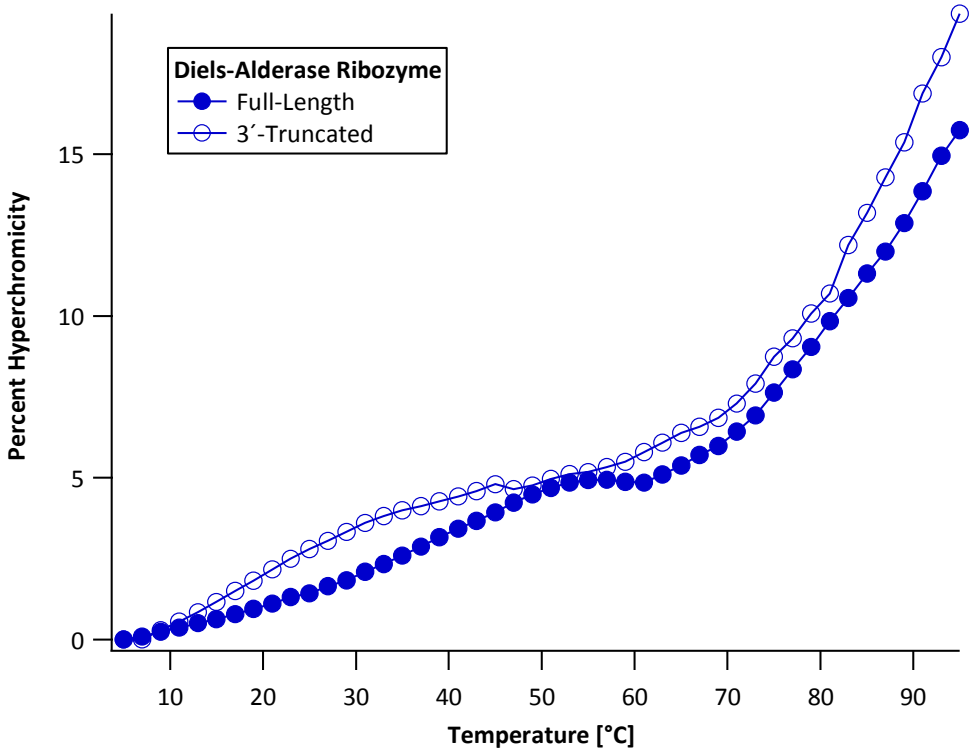

Supplementary Figure S5. Thermal denaturation of full-length and 3′-truncated forms of functional RNAs

All three RNAs studied: malachite green aptamer (red triangles), hammerhead ribozyme (green diamonds), and the Diels-Alderase ribozyme (blue circles) exhibit stabilization of secondary structure in their full-length (filled symbols) forms relative to their primer (3′-truncated) forms (open symbols).

Melt conditions: Malachite green aptamer: Full-length: 5 µM each template and full-length strands, 3′-truncated: 5 µM each template and 3′-truncated strands. Hammerhead: Full-length: 3.75 µM each full-length strand, 3′-truncated: 3.75 µM each 3′-truncated strand. Diels-Alderase: Full-length: 5 µM full-length strand, 3′-truncated: 5 µM 3′-truncated strand. Buffer conditions: 250 mM tris-HCl pH 8, 100 mM NaCl, 1 mM Na-EDTA pH 8. Melts were performed in a 1 mm quartz cuvette (Hellma) using an Agilent Cary 60 interfaced to a Quantum Northwest LC 600. The temperature reported is the block temperature. The background-corrected 260 nm absorbance is reported as percent hyperchromicity at this wavelength relative to the lowest temperature point on the graph. Traces shown are the first cooling trace after a slow heating ramp. All heating and cooling was performed at ≤1°C/min.